Geosynthetics - 7th ICG - Delmas, Gourc & Girard (eds) © 2002 Swets & Zeitlinger, Lisse ISBN 90 5809 523 1

Dynamic model test of express railway subgrades reinforced with geocells

Q. LUO, Y. CAI, X. CAO
School of Civil Engineering, Southwest Jiaotong University, Chengdu, Sichuan, China

ABSTRACT: Full-scale dynamic tests were conducted to evaluate the effects of geocells in the stabilization of railway subgrades in the construction of express railway (with design speed greater than 200 km/h). Four groups of tests with varying heights of geocells (100mm and 150mm) and stabilizing depths (300mm and 600mm) were designed in this research. Stress and deformation data in the subgrade were collected under the application of static and dynamic loads. Test results show: 1)With geocell embedded in the upper layer of subgrade, maximum static and dynamic stresses in the subgrade can be reduced. Deformation can be significantly reduced under static and dynamic load applications. Permanent strain accumulated in the subgrade under repeated loading can be greatly reduced. 2) Strengthening effects of geocells in railway subgrade are proportional to geocell height. 3) With geocell stabilization in subgrade, thickness of granular layer on top of the subgrade can be reduced accordingly.

1 INTRODUCTION

Geocell is a new type of special geosynthetics with three dimensional honeycomb structure composed of belt polymers (usually HDPE, high density polyethylene) through welding using special ultrasonic welders. Compared to conventional plane-type geosynthetics such as geotextile, geomembranes, geonets and geogrids, geocell exhibits better stabilization effectiveness. With coarse granular materials filled in the cells and strong side resistance of cells, geocell together with filled materials can form stable, structural layer and greatly improve mechanistic behavior of stabilized soil.

Due to limited history of geocell development and application, no standards nor specifications of geocells have been organized with respect to design, construction and inspection. Research efforts about geocell stabilization behavior are primarily focused on the material behavior of cells, width and heights of cells, the influence of physical, mechanical properties of filled materials on stabilization effectiveness(Bathurst et al; Mhaiskar et al; Jiang 1996; Ma et al 2000).

Geocell stabilization in railway subgrade is a new technique developed over the last decade. Etsuo Sekine(1994) conducted full-scale static and dynamic model tests of subgrades stabilized with geocells. Xie（1996）、Wang(1998) and Li (2000) conducted field tests of weak subgrade reinforce with geocells.

Full-scale dynamic tests were conducted to evaluate the effects of geocells in the stabilization of railway subgrades in the construction of express railway (with design speed greater than 200 km/h), Qingshen Express Railway from Qinghuangdao, Hebei Province to Shenyang, Liaoning Province. Four groups of tests with varying heights of geocells (100mm and 150mm) and stabilizing depths (300mm and 600mm) were designed in this research. Stress and deformation data in the subgrade were collected under the application of static and dynamic loads using multi-purpose railway testing system. The effectiveness of geocells in subgrade stabilization is evaluated and the influence of subgrade upper layer thickness and geocell heights on subgrade stabilization is analyzed.

2 LABORATORY TESTS

2.1 *Test model*

The model is 7000-mm-long and 4000-mm-wide with varying heights of 1250 ~ 1550 mm. The 1250-mm-high model is composed of 350mm of ballast layer, 300 of granular layer, and 600mm of clayey soil. The 1550-mm-high model is composed of 350mm of ballast layer, 600mm of granular layer, and 600mm of clayey soil. Geocell has two heights: 100m and 150mm, embedded in the middle or upper part of granular layer. Track substructure is constructed with conventional ballast while subgrade layer is composed of granular material in good gradation with silty clay as subsoil fills. Track structure is composed of two reinforced concrete sleepers and two short rails of 50 kg/m with standard gauge of 1435mm to form tie raft with tie spacing of 560mm, which is put directly over the compacted ballast. Additional ballast is filled between ties in turn to the surface of ties. Loading beam is installed in the center of tie raft and connected to the actuator in the fatigue testing system, PME-100. The actuator is able to provide sinusoid load wave with a frequency ranging from 0~8Hz and an amplitude between 0~250kN. Figure 1 illustrates test configuration in detail.

2.2 *Instrumentation*

Instrumentation was design in the four layers of the model tests as presented in Figure 1. The four instrumented layers situated at the top of the subgrade (A-A), middle of the subgrade layer (B-B), top of subsoil fill (C-C) and middle of fill (D-D), with vertical distance of 0, 300mm, 600mm, and 900mm from the top of the subgrade layer, respectively. Seven points: ①, ②, ③, ④, ⑤, ⑥ and ⑦ were selected to place sensors in accordance with measuring purposes with points of ①, ②, ④ and ⑥ located at the cross points between rails and ties, point ⑤ situated in the middle of the ties and points ③ and ⑦ outside of the two ends of ties, as presented in Table 1.

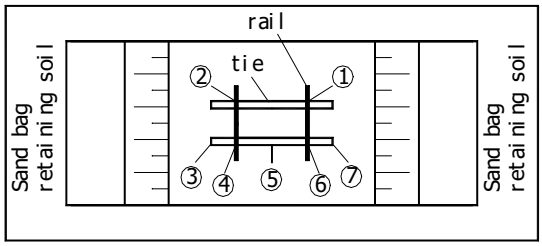

(a) Plan view

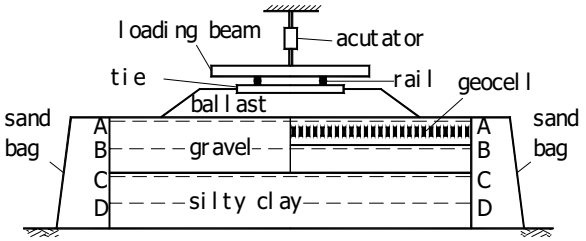

(b) Side view
Figure 1. Model test configuration

Table 1. Instrumentation plan

location	Pressure cell	LVDT
A-A	①②③④⑤⑥⑦	②
B-B	①②③④⑤⑥⑦	①
C-C	①②④⑥	④
D-D	①	⑥

2.3 *Material Properties*

Track substructure is constructed using conventional railway ballast. Upper layer of subgrade is constructed using gravels with good gradation. Figure 2 illustrates the gradation curve. Silty clay is used in the under upper layer of subgrade with material properties listed in Table 2.

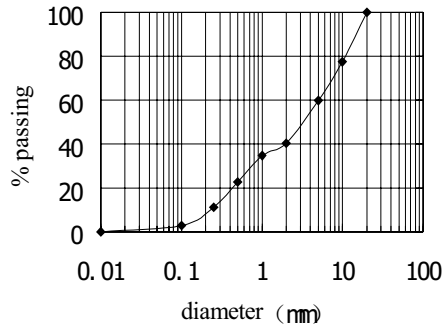

Figure 2. Gradation curve of gravels

Table 2. Soil properties

G_S	w_{opt} (%)	$\rho_{d\max}$ (kN/m^3)	w_P (%)	w_L (%)
2.72	13.89	17.4	15.6	32.0

Geocell is made of (HDPE) with a film thickness of 1.25mm, tension strength greater than 21MPa, low-temperature britlle point less than -50^{0}C, environmental cracking resistance period longer than 100h, room temperature welding strength greater than 10N/mm and expanded nets of 210mm × 220mm as illustrated in Figure 3. Geocells used in the test is black.

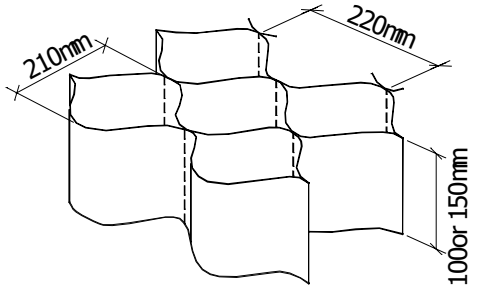

Figure 3. Structure of Geocell

2.4 *Test design*

Four groups of test were conducted to simulate the influence of variation in thickness of subgrade layer and heights of geocells on the behavior of stress and deformation of subgrade under static and dynamic load application. Table 3 precents the combination of subgrade layer thickness and geocell heights used in laboratory investigation.

Table 3. Configuration of layer and geocell heights (mm)

Group No.	Ballast thickness	Upper layer of subgrade	Embankment fill	Geocell heights
1	350	600	600	No geocell
2	350	600	600	100
3	350	300	600	100
4	350	600	600	150

2.5 *Loading process*

Loading process is outlined as follows. 1)Static loading. Loading is increased from 0 to 140kN with a loading step of 20kN. Loading is gradually increased after stable deformation exhibits under previous loading state. 2)Dynamic loading. A static loading of 20kN is initially applied as the lower limit of dynamic loading and gradually increased to 140kN as the upper limit with a loading step of 20 kN over 500 load repetitions for each loading step. 3)Repeated load tests with 1,500,000 repetitions. Dynamic loading is applied at 20～140kN with a frequency of 5Hz and repetitions of 1,5000,000.

3 TEST RESULTS

3.1 *Test state*

K_{30} values at the top, middle and bottom of subgrade layer were measured in the preparation of test model as listed in Table 4. Compacted densities in corresponding layers were recorded using CPN MC-3 nuclear gauge as presented in Table 5.

K_{30} values of granular layers in the 4 groups of model tests vary between 208～227MPa/m with an average of 218MPa/m and a difference of 19MPa/m. K_{30} values of silty clay fill under subgrade layer vary between 175～178MPa/m with an average of 176MPa/m and a difference of 3MPa/m.

Compacted densities granular layers in the 4 groups of model tests vary between 21.7～22.1kN/m^3 with an average of 21.94 kN/m^3 and a difference of 0.04 kN/m^3. Compacted densities of silty clay fill under subgrade layer vary between 19.3～19.5kN/m^3 with an average of 19.43 kN/m^3, a difference of 0.02 kN/m^3 and compaction coefficients greater than 0.97

Based on test data in Table 4 and Table 5, it can be seen that subgrades in tests of group 2, group 3, and group 4 have higher K_{30} value with lower compacted densities, compared to those in group 1. It can be concluded that subgrade exhibits an increase in strength and stiffness after stabilization with geocell.

Table 4. K_{30} Value in subgrade (MPa/m)

location	Group 1	Group 2	Group 3	Group 4
Top of subgrade	208	216	222	214
Middle of subgrade	227	223	/	220
Top of embankment fill	175	175	177	178

Table 5. Compacted unit weight of subgrade（kN/m^3）

Location	Group 1	Group 2	Group 3	Group 4
Top of subgrade	22.1	21.9	21.9	21.7
Middle of subgrade	22.1	22.1	/	21.8
Top of embankment fill	19.4	19.5	19.3	19.5

3.2 *Static test*

3.2.1 *static stress*

Static stress exhibits linear relationship with applied loading. With a static load of 140kN,the average stress observed in points ①, ②, ④ and ⑥ in each layer is listed in Table 6. Test results show that dynamic stress has been reduced to different scale in subgrade layers with geocell embedded. Static stresses at the top of subgrade (A-A layer) in model tests of group 2, group 3, and group 4 with geocell stabilization were reduced to 94.9%, 90.1% and 91.2%, respectively, compared to that in group 1 test without geocell stabilization. Static stresses in the middle of B-B layer in tests of group 2, group 3, and group 4 were found to be 83.14%, 97.97% and 78.78% of that in group 1 test, respectively. Static stresses in layers under C-C plane were fairly stable with small reduction.

Table 6. Static stress in subgrade (kPa)

Location	Group 1	Group 2	Group 3	Group 4
A-A	56.7	53.8	51.1	51.7
B-B	34.4	28.6	33.7	27.1
C-C	17.9	17.2	19.2	13.3
D-D	6.8	7.1	/	5.2

3.2.2 *static deformation*

Static deformation produced in subgrade layers is linear with static loading (ballast exhibits non-linearity relationship). Table 7 presents static deformation data observed in subgrade layers under a 140kN of static load application. Test results show that static deformation has been reduced to different scales in subgrade layers with geocell embedded. Static deformations at the top of subgrade (A-A layer) in model tests of group 2, group 3, and group 4 with geocell stabilization were reduced to 78.4%、91.3% and 61.0%, respectively, compared to that in group 1 test without geocell stabilization. Static deformations in the middle of B-B layer in tests of group 2, group 3, and group 4 were found to be 81.0%, 93.8% and 82.0% of that in group 1 test, respectively. Static deformation in layers under C-C plane were fairly stable with small reduction.

Table 7. Static deformation in subgrade (mm)

Location	Group 1	Group 2	Group 3	Group 4
A-A	0.574	0.450	0.524	0.35
B-B	0.305	0.247	0.286	0.25
C-C	0.183	0.130	/	0.16

Table 8 lists compressive deformation data in subgrade layers with a static load of 140kN. Test results show that compressive deformation has been reduced to different extents in subgrade layers with geocell embedded. Compressive deformations in the upper layer of subgrade in model tests of group 2, group 3, and group 4 with geocell stabilization were reduced to 75.46%, 88.48% and 37.17%, respectively, compared to that in group 1 test without geocell stabilization. Compressive deformations in the lower subgrade layer in tests of group 2 and group 4 were found to be 95.9% and 73.77% of that in group 1 test, respectively.

Table 8. Compressive deformation in subgrade (mm)

Location	Group 1	Group 2	Group 3	Group 4
Upper layer of subgrade	0.269	0.203	0.238	0.1
Lower layer of subgrade	0.122	0.117	/	0.09

Based on analysis stated above, it can be concluded that geocell-stabilized subgrade under static load application reduces static stress and static deformation in the upper layer of subgrade. Reduction of static stress and static deformation in the lower part of subgrade is also expected. The higher the geocells, the greater the effectiveness in stabilization.

3.3 *Dynamic tests*

3.3.1 *dynamic stress*

Dynamic stress in subgrade layers in the model tests has a linear relationship with dynamic loading. With an application of dynamic loading of 20kN～140kN, the average dynamic stress of points ①, ②, ④ and ⑥ in subgrade layers is listed in Table 9. Test results show that dynamic stress has been reduced to different scale in subgrade layers with geocell embedded. Dynamic stresses at the top of subgrade (A-A layer) in model tests of group 2, group 3, and group 4 with geocell stabilization were reduced to 94.4%, 89.4% and 82.2%, respectively, compared to that in group 1 test without geocell stabilization. Dynamic stresses in the middle of B-B layer in tests of group 2, group 3, and group 4 were found to be 77.3%, 90.6% and 67.1% of that in group 1 test, respectively. Dynamic stresses in layers under C-C plane were fairly stable with small reduction.

Table 9. Dynamic stress in subgrade(kPa)

location	Group 1	Group 2	Group 3	Group 4
A-A	69.75	65.84	62.39	57.32
B-B	42.58	32.92	38.59	28.55
C-C	19.04	18.47	19.52	16.07
D-D	9.65	9.12	/	8.52

3.3.2 *resilient deformation*

Resilient deformation is caused by wheel loading of traveling vehicles. Primary resilient deformation occurs in upper layer of subgrade. Resilient deformation produced in subgrade will ultimately constitute a significant part in the resilient deformation occurred in rail surface. Train speed will be limited by great resilient deformation. Meanwhile, reduction in resilient deformation in subgrade can reduce maintenance work of track structure.

Resilient deformation is found to be linear with loading amplitude (difference between upper limit and lower limit of dynamic loading). Table 10 lists resilient deformation with dynamic loading amplitude varying from 20kN ~ 140kN. Compared to group 1 test without geocell stabilization, group 2 test with 100mm-high geocell stabilization produces smaller resilient deformation at the top of subgrade (A-A layer) with a reduction of 15.9% while resilient deformation in group 4 test with 150mm-high geocell stabilization is reduced to 78.6%. Geocell-stabilized subgrade has better deformation resistance behavior, and resilient deformation reduction is in proportion to geocell height.

Compared with group 1 model test of 600mm granular layer and no geocell stabilization, group 3 test with 100mm-high geocell stabilization produces 11.9% smaller resilient deformation at the top of subgrade (A-A layer) even if the thickness of granular layer is reduced to 300mm. It can be concluded that geocell stabilization is efficient and resilient deformation in the subgrade can be controlled in the thinner granular layer subgrade with geocell reinforcement.

Table 10. Elastic deformation in subgrade (mm)

location	Group 1	Group 2	Group 3	Group 4
A-A	0.542	0.456	0.478	0.426
B-B	0.43	0.366	0.398	0.321
C-C	0.23	0.21	/	0.159

3.4 *Repeated loading test*

Relationship between accumulated deformation and load repetitions exhibits linearity in log-log scale. Accumulated deformation in subgrades is listed in Table 11 with 5Hz of frequency and 20~140kN of dynamic loading over 1,500,000 repetitions.

Deformation at the top of subgrade is the summation of deformation accumulated over all layers. After 1,500,000

repetitions, Accumulated deformation at the top of subgrade (A-A layer) in model tests of group 2, group 3, and group 4 with geocell stabilization were reduced to 41.4%、48.3% and 33.0%, respectively, compared to that in group 1 test without geocell stabilization. Accumulated deformation in B-B layer in tests of group 2, group 3, and group 4 were found to be 47.8%, 63.2% and 50.9% of that in group 1 test, respectively. All these indicate that geocell stabilization can effectively reduce subgrade deformation.

With the thickness of granular layer subgrade reduced, improved deformation behavior was also observed in the test of group 3 reinforced with geocells compared to test results in the test of group 1 having greater granular layer subgrade thickness without geocell stabilization. It can be concluded that geocell stabilization in the thinner granular layer subgrade is an effective alternative in the design of railway subgrade.

Table 11 Accumulated deformation in subgrade(mm)

location	Group 1	Group 2	Group 3	Group 4
A-A	2.118	0.877	1.023	0.699
B-B	1.023	0.489	0.647	0.521

4 CONCLUSION

1)With geocell embedded in the upper layer of subgrade, maximum static and dynamic stresses in the subgrade can be reduced. Deformation can be significantly reduced under static and dynamic load applications. Permanent strain accumulated in the subgrade under repeated loading can be greatly reduced. As suggested by test data in group 1 and group 2 model tests, static stress and dynamic stress in subgrade reinforced with 100m-high geocells can be reduced by 5% and 6%, respectively, with 22% reduction in static deformation, 16% reduction in dynamic deformation and 59% reduction in accumulated vertical strain.

2) Strengthening effects of geocells in railway subgrade are proportional to geocell height. With geocell height increased from 100mm to 150mm, 4% and 12 % reduction in static and dynamic stress in subgrade were observed, respectively, as indicated by test results of group 2 and group 4. At the same time, 17% reduction in static deformation was recorded along with 5% reduction in dynamic deformation and 8% reduction in accumulated deformation.

3) With geocell stabilization in subgrade, thickness of granular layer subgrade can be reduced accordingly. With gravel thickness decreased from 600mm to 300mm, static stress and dynamic stress in subgrade reinforced with 100mm-height geocells can be reduced by 10% and 11%, respectively, as supported by test results of group 1 and group 3. Also observed are 9% reduction in static deformation, 12% reduction in dynamic deformation and 52% reduction in accumulated strain.

REFERENCE

Bathurst, R. J et al. Large-Scale Model Tests of Geocomposite Mattresses Over Peat Subgrades. Transportation Research Record, No.1188: 28-36

Bathurst, R. J et al. Large-Scale Triaxial Compression Testing of Geocell-Reinforced Granular Soils. Geotechnical Testing Journal, Vol.16, No.3: 296-303

Mhaiskar, S. Y et al. Soft Clay Subgrade Stabilisation Using Geocell. Pro. of the 1992 ASCE Specialty Conference on Grouting, Soil Improvement and Geosynthetics, New Orleans, LA, USA

Jiang huihuang. 1996. Model test and analysis of geocell-stabilized railway subgrades, Master thesis, Academy of Railway Science of China (in Chinese).

Ma zhuojun et al. 2000. Strength behavior of geocell-reinforced clay. Highway, No.10: 34-35 (in Chinese)

Etsuo Sekine et al. 1994. Study on Properties of Road Bed Reinforced with Geocell. Quarterly Reporties of RTRI(Japan), 35(1): 23-31

Xie Qixin. 1996. Application of geosynthetics in railway subgrades, Proceedings for the 4th Conference of Geosynthetics in China, Shanghai: 340-344 (in Chinese).

Wang Binglong et al.. 1998. Dynamic stress in geocell-stabilized railway subgrades, Journal of Railway, 20(5): 103-108 (in Chinese).

Li Dingqing. 2000. Deformations and Remedies for Soft Railway Subgrades Subjected to Heavy Axle Load. Geotechnical Special Publication, ASCE, USA, No.103: 307-321